MELTING, CRYSTALLIZATION AND MORPHOLOGICAL MODIFICATIONS OF BIODEGRADABLE POLYESTERS IN DENSE CARBON DIOXIDE

Shinya Takahashi and Erdogan Kiran*

Department of Chemical Engineering
Virginia Polytechnic Institute and State University
Blacksburg, VA 24061, USA

Email: ekiran@vt.edu

Abstract. The melting temperature depression, crystallization, and morphological modifications have been investigated for a biodegradable polyester poly(3-hydroxybutyrate-*co*-3-hydroxyvalerate) (PHBV) in the presence of CO_2. Experiments have been carried out in a special variable-volume view cell that permits investigations using thin polymer films. Melting temperature depressions were determined at pressures up to 35 MPa by monitoring the changes in the transmitted light intensities. Morphological modifications that develop were explored at pressures up to 24MPa. These evaluations were carried out by investigations of the changes in the thin films that were melt-crystallized in the view cell using a polarized optical microscope. These films display banded spherulitic morphologies. These banded spherulites are found to display radially oriented pores in the bands which themselves consist of the radially oriented lamellae. The formation of these oriented pores may be the result of the exclusion of CO_2 from the crystal growth front to the amorphous region in between the bundles of the lamellar stacks.

Keywords: Melting temperature depression, Poly(3-hydroxybutyrate-*co*-3-hydroxyvalerate), Carbon dioxide, Crystalline morphology

1. Introduction

The use of dense or supercritical fluids, especially CO_2 at high pressures as a process or processing fluid for polymers is of continuing interest for applications pertaining to formation of particles [1, 2], foams [2-4], fibers [5, 6], or porous structures [7-9]. Especially important in many of these applications is the reduction of the melting or the glass transition temperature [10-24] offering opportunities for processing at lower temperatures which is of great value for processing of polymers that may have a tendency to undergo thermal degradation. One such polymer is poly(3-hydroxybutyrate-*co*-3-hydroxyvalerate) (PHBV) that is known to undergo significant reduction in molecular weight and thus deterioration of its physical properties if processed at temperatures above its ambient melting temperature [25]. We have recently shown that this problem can be potentially alleviated if the polymer were processed in dense CO_2 media which significantly lowers the melting temperature [21].

When exposed to CO_2, in addition to depression of the transition temperatures, semicrystalline polymers undergo also morphological modifications. Dissolving CO_2 enhances the chain mobility which leads to the decreases in the melting temperature and the glass transition temperature of polymers. The enhanced chain mobility also leads to changes of the crystallization kinetics and thus changes in the resultant crystalline morphology. Mechanistically, an important factor to recognize is the faith of CO_2 as the polymer crystallizes. Once the crystallization of the polymer containing CO_2 starts at a given crystallization temperature, the CO_2 is excluded from the growth front of the crystals, and directed to the amorphous regions [26, 27]. This kind of exclusion of impurities during crystallization can be and is observed in other systems, such as the binary systems of crystalline polymer / diluent [28-31] as well as crystalline polymer / amorphous polymer systems [32-37]. This exclusion phenomenon leads to a concentration gradient [38] at the growth front in the "polymer / non-crystalline component" systems undergoing crystallization which is different from that observed in neat

polymer systems. The end result is the observation of altered crystalline morphologies. Indeed, unique crystallization behavior and morphology development in CO_2 has been reported for example in connection with the transition of crystalline forms in syndiotactic-polystyrene [39], thickening of crystalline lamellae in poly(ε-caprolactone) (PCL) [40, 41], the development of nano-rod crystals at the temperatures below the original T_g of poly(L-lactide) [42] or formation of the unique crystalline morphology in isotactic-polypropylene [43].

PHBV is a biodegradable semicrystalline polyester. It is naturally synthesized by microorganisms and accumulated as intracellular materials [44-46]. The exceptional stereoregularity and the high purity due to its natural origin make this polyester an ideal system for the study of hierarchical crystalline morphology, i.e. spherulites. Low nucleation density due to the absence of the impurities allows uncommonly large spherulites to grow during crystallization from the melt [47-49]. At a certain temperature range, the spherulites exhibit the concentric alternating extinction banded pattern observed under a cross-polarized optical microscope. Generally, the band spacing increases with increasing crystallization temperature. This banded pattern is attributed to the helicoidal twisting of the radial lamellar crystals [50, 51]. With respect to the surface topology, a study conducted by atomic force microscopy (AFM) shows that the banded spherulites consist of concentric ridges and valleys having around 100 nm vertical distances [52]. Moreover, it is also found that the ridge area is constituted of edge-on lamellae aligned to the radial direction of the spherulites while the valley area is formed by flat-on lamellae.

In the present paper, we report on the crystallization and morphological modifications of PHBV in CO_2. The melt-crystallization of PHBV was conducted in CO_2 up to 24 MPa at 90 °C and 100 °C. The crystalline morphologies obtained were characterized by a cross-polarized microscope. A mechanism for the formation of the observed morphologies is proposed which is based on the concept of exclusion of CO_2 from the crystals during crystallization.

2. Experimental Methods and Procedures

2.1 Material characterization

CO_2 (Airgas) with a purity of 99.9995% was used in this study. PHBV (HV content = 12 wt%) was purchased from Sigma-Aldrich Co. Because as-received PHBV contained some impurities which could not be dissolved in chloroform, the polymer was purified by first dissolving in chloroform (to remove the undissolved impurities) and then reprecipitation in methanol. The molecular weights of the purified PHBV were M_w = 250,000 and M_n = 100,000 g/mol.

2.2 Experimental system

Figure 1 shows a schematic diagram of the experimental system. The details have been provided in a recent publication [21]. Briefly, it is a variable volume view-cell equipped with sapphire windows and a movable piston. Two sapphire windows are set 25.4 mm apart in the opposite side of the view-cell and provide a 25.4 mm diameter full view of the cell interior for visual observation and/or optical recording of the transmitted light intensities. The position of the piston is monitored with a position sensing liner variable differential transformer (LVDT). Pressures and temperatures inside the view-cell are measured with a Dynisco flush-mount sensor with an accuracy of ± 0.5 °C, and ± 0.1 MPa, respectively.

The inside cavity of cell is especially designed with a 25.4 × 25.4 mm square-shaped cross section which facilities the easy positioning of the sample holders that are used in the present study. Figure 2 shows photographs of the sample holders for the melting and the crystallization studies. The sample holder for the melting study is made of an aluminum block with a slit in which the polymer film in between two microscope slides is vertically inserted. The assembly is then put inside the cell with a full view of the film across the sapphire windows. The sample holder for the investigation of morphological changes after melt-crystallization is also an aluminum block, but now with a flat, depressed rectangular cavity region on the top surface that permits placement of a thin film with a cover glass in a horizontal geometry.

2.3 Experimental procedures for crystallization and morphological characterization

Sample preparation. Thin film samples of PHBV with 20 μm of thickness were prepared by solution casting of 1 wt % solutions in chloroform on a glass dish. The solvent was then allowed to evaporate at room

temperature in atmosphere for 24 h. The film was further dried at 50 °C for 48 h in the vacuum oven.

Procedure for the crystallization of PHBV in air at ambient pressure. The thin PHBV film on a cover glass was placed on a hot stage at 192 °C for 1 min. Subsequently, the sample was transferred onto another hot stage set at target crystallization temperatures in the range from 70 to 120 °C.

Procedure for the crystallization of PHBV in CO_2. The thin film was placed horizontally using the special sample holder (see Figure 1b) in the view cell. The cell was then charged with CO_2. The temperature and the pressure of the cell were increased to 142 °C and 28 MPa, and held there for 30 min for the initial absorption of CO_2 in the film. Then, the cell was further heated up to 162 °C, which was 20 °C higher than the melting temperature at the pressure, and held for an additional 30 min for complete melting. Subsequently, the cell was cooled to a desired temperature (in the range 90 - 100 °C) and pressure (5 - 24 MPa) for the crystallization of the film to take place. After the crystallization, the cell was depressurized and the film was taken out from the cell. The crystallized film was kept at -5 °C, which is 10 °C lower than the glass transition temperature of PHBV until morphological characterizations were carried out.

Polarized optical microscopy. A polarized optical microscope (OMAX M837PL) equipped with a digital camera was used to analyze the crystalline morphology of the crystallized samples. In order to obtain the information of birefringence, a sensitive tint plate having an optical path difference of 530 nm was inserted between the samples and analyzer.

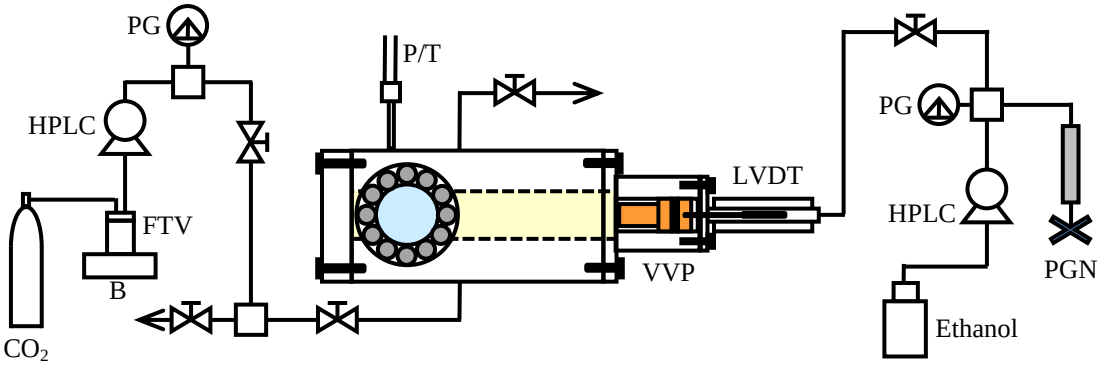

Figure 1. Schematic diagram of the view-cell. HPLC: HPLC pump; PG: pressure gauge; P/T: pressure and temperature sensor; FTV: fluid transfer vessel; VVP: variable volume part housing the movable piston; LVDT: linear variable differential transformer; PGN: pressure generator.

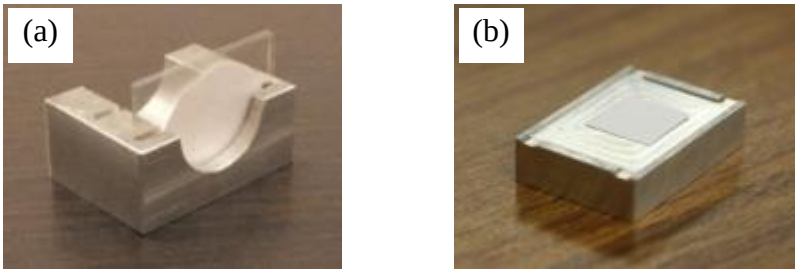

Figure 2. Pictures of the sample holders for (a) *in-situ* determination of the melting temperature from changes in transmitted light intensity, and (b) for crystallization and post assessment of the morphology under a polarized microscope.

3. Results and discussion

3.1 Melting behavior and melting temperature depression of PHBV in CO_2 at high pressure

We have recently reported on the melting behavior and the melting temperature depression in PCL, poly(3-hydroxybutyrate), and PHBV using the present experimental system [21]. Since details have already been published, below we are providing some salient features for PHBV only. Figure 3 shows the DSC

thermogram of PHBV at ambient pressure (conducted using a Perkin-Elmer Pyris Diamond DSC), and the transmitted light intensity scan conducted in the present view cell at ambient pressure. The DSC thermogram shows a double melting peak, and likewise the transmitted light intensity curve shows a two-step increase in the transmittance reflecting the two-stage nature of the melting process. Figure 4 shows the transmitted light intensity scans conducted in CO_2 by increasing the temperature while holding the cell volume constant, which shows the pressures at which the melting transitions occur. The complete melting temperatures, T_m, and pressures were identified as the end point of the change in the transmitted light intensities. These are plotted in Figure 5, which shows the melting temperature as a function of pressure.

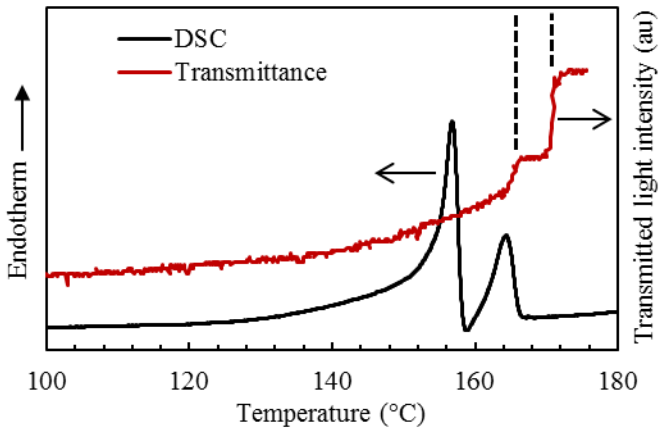

Figure 3. DSC thermogram in N_2 and transmitted light intensity of PHBV at ambient pressure.

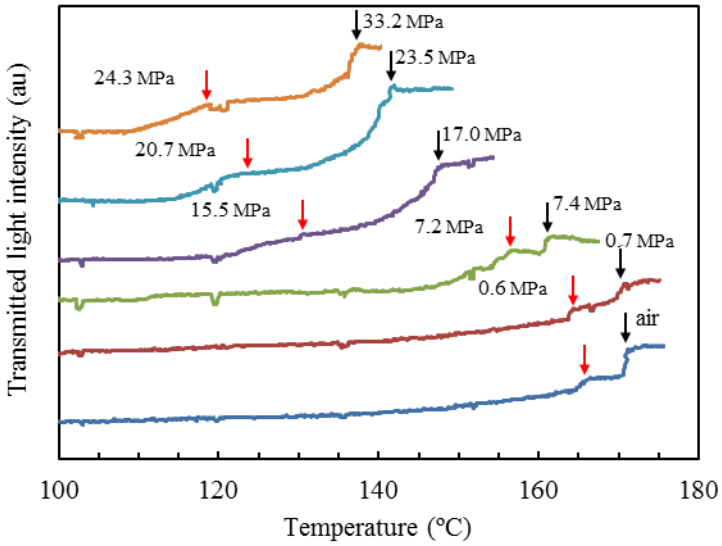

Figure 4. Variation of transmitted light intensities of PHBV with temperature/pressure in CO_2.

As shown in the figure, T_m shows a linear decrease with increasing pressure up to about 24 MPa. At higher pressures, rate of reduction in T_m is not high. This behavior is a consequence of the pressure dependence of the solubility of CO_2 in the polymer [21]. At pressures below 24 MPa, CO_2 rapidly dissolves in the polymer. The solubility of CO_2 increases with pressure and leads to the significant reduction (at a rate of about -1.3 °C/MPa) in the melting temperature. At pressures above 24 MPa, solubility of CO_2 does not increase much, while the hydrostatic pressure effect starts to become more prevalent balancing the solubility effect. As

a result the melting temperature depression tends to level off. As shown in the figure, for PHBV, a melting temperature reduction as high as 34 °C can be achieved.

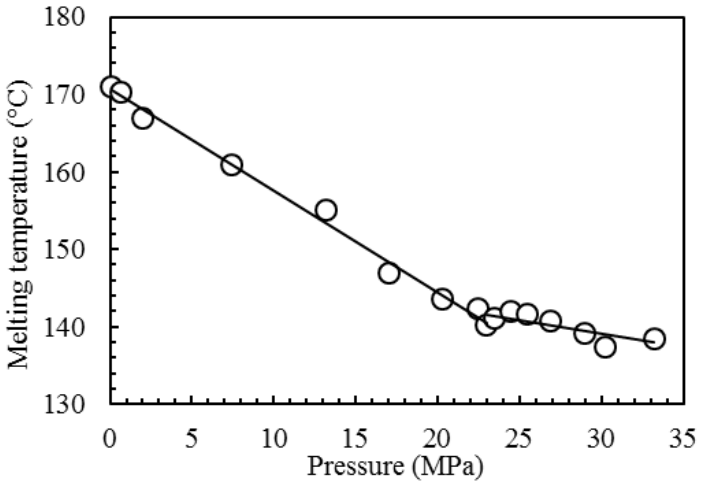

Figure 5. Melting temperature depression of PHBV as a function of CO_2 pressure.

3.2 Crystalline morphology of PHBV melt-crystallized in CO_2

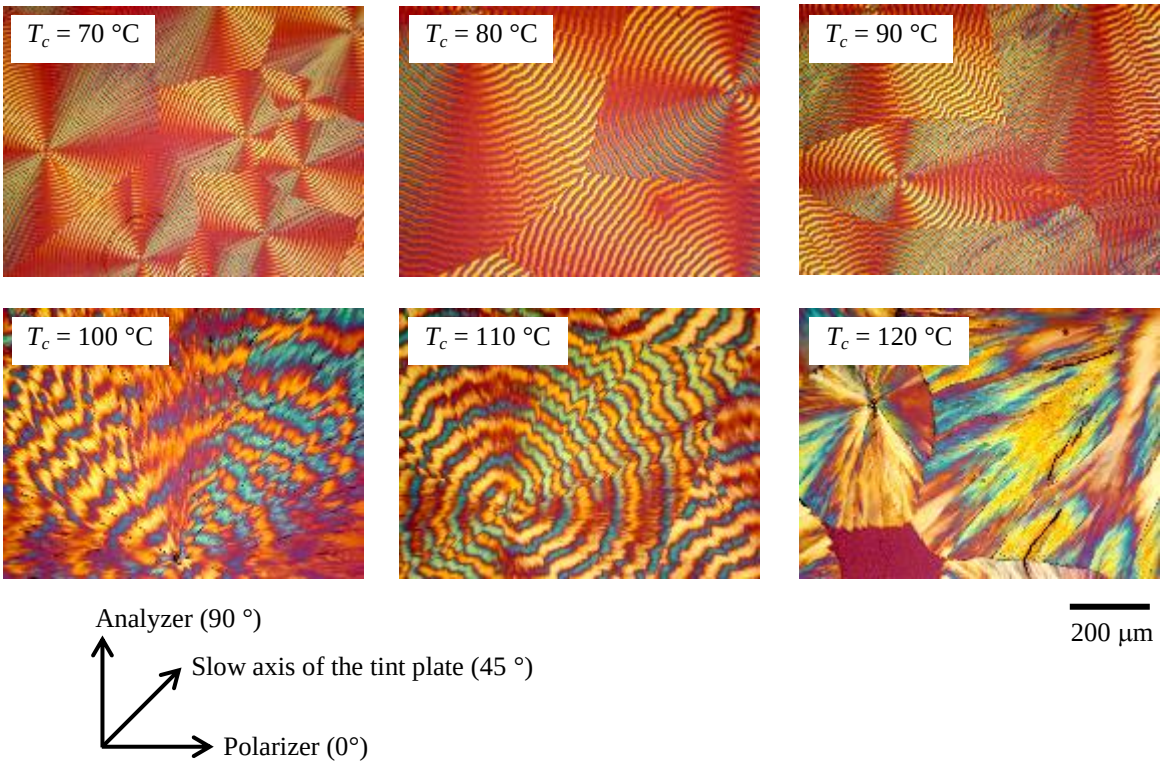

Figure 6. Cross-polarized micrographs of PHBV crystalized in air at ambient pressure at various temperatures.

Figure 6 shows the cross-polarized optical micrographs of PHBV crystallized in air at ambient pressure. Double ring-banded spherulites are seen in the polymer crystallized at temperatures below 110 °C. With increasing crystallization temperature, T_c, the spherulite radius and the band spacing increase, and the

regularity of the band pattern becomes coarse. The color variation of the micrographs reveals the information of lamellae orientation. Because the refractive index in the chain direction of PHBV is smaller than that in its vertical direction due to the large polarizability anisotropy of the carbonyl groups which are oriented in the vertical direction to the main chain direction, the intrinsic birefringence of the PHBV crystal shows a negative value [53]. This means the refractive index along the width and the length direction of the lamella of PHBV is larger than that along the thickness direction. If the direction having the largest refractive index in the lamella is parallel to the slow axis of the tint plate (direction showing the largest refractive index in the tint plate) which is at 45 ° of the azimuthal angle in this study, the region colors blue. Conversely, if the same direction is perpendicular to the slow axis of the tint plate, the region becomes yellow. Hence, the blue-colored bands in the first and the third quadrants and the yellow-colored bands in the second and the forth quadrants are attributed to the radial orientation of the edge-on lamellae.

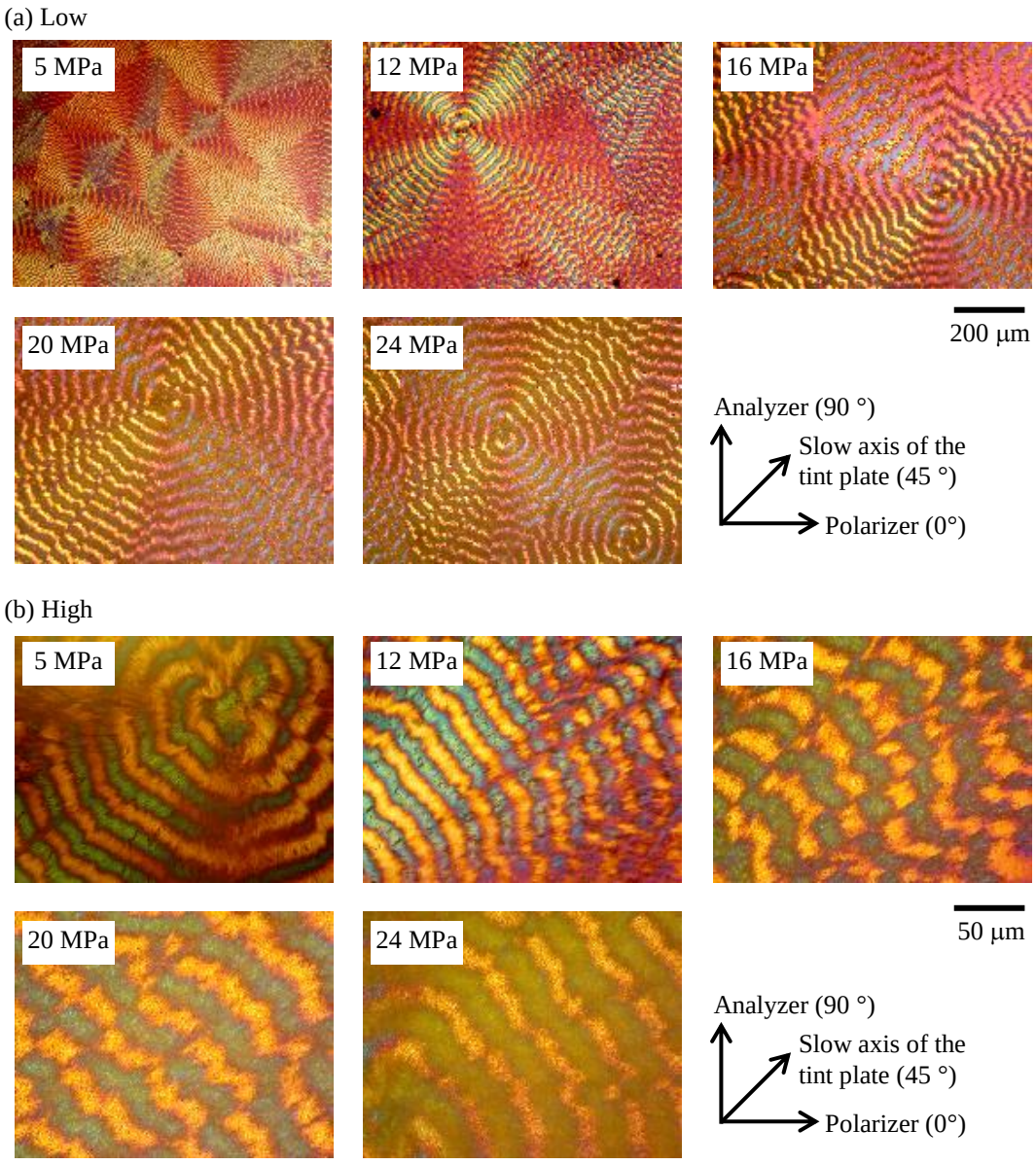

Figure 7. Cross-polarized micrographs with (a) low magnification and (b) high magnification of PHBV crystalized at 90 °C in CO_2 of various pressure.

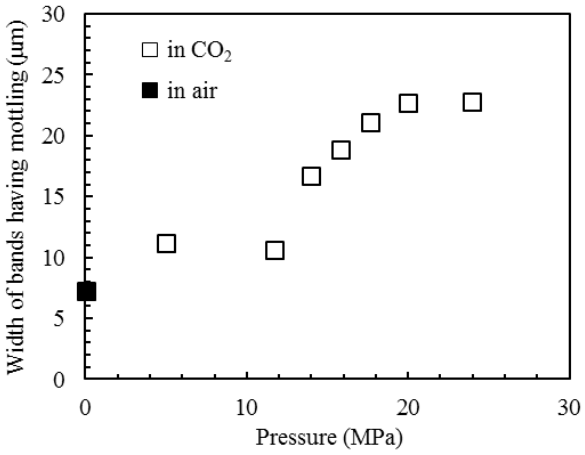

Figure 8. Width of the bands having the mottling in spherulites formed in CO_2. For comparison, the bands width crystallized at 90 °C under ambient pressure is also shown in the figure.

4. Conclusion

The melting temperature of PHBV shows a linear decrease up to 24 MPa, leading to a decrease of about 34 °C in T_m. Crystallization of PHBV in CO_2 at high pressures leads to banded spherulites having radially-oriented pores in the bands which consist of the lamellae aligned to the radial direction of the spherulites. CO_2 is excluded from the crystal growth front and moves into the amorphous region in between bundles of the lamellar stacks leading to the formation of pores.

Acknowledgement

This research has in part been supported by Kureha Corporation, Japan.

References

[1] S.-D. Yeo, E. Kiran, Formation of polymer particles with supercritical fluids: a review, Journal of Supercritical Fluids 34 (2005) 287-308.
[2] S.P. Nalawade, F. Picchioni, L.P.B.M. Janssen, Supercritical carbon dioxide as a green solvent for processing polymer melts: processing aspects and applications, Progress in Polymer Science 31 (2006) 19-43.
[3] E. Kiran, Polymer miscibility, phase separation, morphological modifications and polymorphic transformations in dense fluids, Journal of Supercritical Fluids 47 (2009) 466-483.
[4] M. Sauceau, J. Fages, A. Common, C. Nikitine, E. Rodier, New challenges in polymer foaming: a review of extrusion processes assisted by supercritical carbon dioxide, Progress in Polymer Science 36 (2011) 749-766.
[5] M.J. Meziani, P. Pathak, W. Wang, T. Desai, A. Patil, Y.-P. Sun, Polymeric nanofibers from rapid expansion of supercritical solution, Industrial and Engineering Chemistry Research 44 (2005) 4594-4598.
[6] Wahyudiono, K. Murakami, S. Machmudah, M. Sasaki, M. Goto, Production of nanofibers by electrospinning under pressurized CO_2, High Pressure Research: An International Journal 32 (2012) 54-59.
[7] A.R.C. Duarte, J.F. Mano, R.L. Reis, Supercritical fluids in biomedical and tissue engineering applications: a review, International Materials Reviews 54 (2009) 214-222.
[8] Fanovich, P. Jaeger, Sorption and diffusion of compressed carbon dioxide in polycaprolactone for the development of porous scaffolds, Materials Science and Engineering C 32 (2012) 961-968.
[9] L.J.M. Jacobs, M.F. Kemmere, J.T.F. Keurentjes, Sustainable polymer foaming using high pressure carbon dioxide: a review on fundamentals, processes and applications, Green Chemistry 10 (2008) 731-738.
[10] E. de Paz, Á. Martin, S. Rodríguez-Rojo, J. Herreras, M.J. Cocero, Determination of phase equilibrium (solid-liquid-gas) in poly-(ε-caprolactone) - carbon dioxide systems, Journal of Chemical & Engineering Data 55 (2010) 2781-2785.
[11] K. Fukné-Kokot, A. König, Ž. Knez, M. Škerget, Comparison of different methods for determination of the S-L-G equilibrium curve of a solid component in the presence of a compressed gas, Fluid Phase Equilibria 173 (2000) 297-310.

[12] M. Karimi, M. Heuchel, T. Weigel, M. Schossig, D. Hofmann, A. Lendlein, Formation and size distribution of pores in poly(ε-caprolactone) foams prepared by pressure quenching using supercritical CO_2, Journal of Supercritical Fluids 61 (2012) 175-190.
[13] Ž. Knez, M. Škerget, Z. Mandžuka, Determination of S-L phase transitions under gas pressure, Journal of Supercritical Fluids 55 (2010) 648-652.
[14] B. Li, X. Zhu, G.-H. Hu, T. Liu, G. Cao, L. Zhao, W. Yuan, Supercritical carbon dioxide-induced melting temperature depression and crystallization of syndiotactic polypropylene, Polymer Engineering & Science 48 (2008) 1608-1614.
[15] L. Li, T. Liu, L. Zhao, W.-k. Yuan, Effect of compressed CO_2 on the melting behavior and βα-recrystallization of β-form in isotactic polypropylene, Journal of Supercritical Fluids 60 (2011) 137-143.
[16] Z. Lian, S.A. Epstein, C.W. Blenk, A.D. Shine, Carbon dioxide-induced melting point depression of biodegradable semicrystalline polymers, Journal of Supercritical Fluids 39 (2006) 107-117.
[17] A. Serbanovic, Ž. Petrovski, M. Manic, C.S. Marques, G.V.S.M. Carrera, L.C. Branco, C.A.M. Afonso, M. Nunes da Ponte, Melting behaviour of ionic salts in the presence of high pressure CO_2, Fluid Phase Equilibria 294 (2010) 121-130.
[18] S.L. Shenoy, T. Fujiwara, K.J. Wynne, Quantifying plasticization and melting behavior of poly(vinylidene fluoride) in supercritical CO_2 utilizing a linear variable differential transformer, Macromolecules 36 (2003) 3380-3385.
[19] M. Takada, S. Hasegawa, M. Oshima, Crystallization kinetics of poly(L-lactide) in contact with pressurized CO_2, Polymer Engineering & Science 44 (2004) 186-196.
[20] M. Türk, G. Upper, P. Hils, Formation of composite drug-polymer particles by co-precipitation during the rapid expansion of supercritical fluids, Journal of Supercritical Fluids 39 (2006) 253-263.
[21] S. Takahashi, J.C. Hassler, E. Kiran, Melting behavior of biodegradable polyesters in carbon dioxide at high pressures, Journal of Supercritical Fluids 72 (2012) 278-287.
[22] E. Weidner, V. Wiesmet, Ž. Knez, M. Škerget, Phase equilibrium (solid-liquid-gas) in polyethyleneglycol - carbon dioxide systems, Journal of Supercritical Fluids 10 (1997) 139-147.
[23] Z. Zhang, Y.P. Handa, CO_2-assisted melting of semicrystalline polymers, Macromolecules 30 (1997) 8505-8507.
[24] P.D. Condo, I.C. Sanchez, C.G. Panayiotou, K.P. HJohnston, Glass transition behavior including retrograde vitrification of polymers with compressed fluid diluents, Macromolecules 25 (1992) 6119-6127.
[25] M. Kunioka, Y. Doi, Thermal degradation of microbial copolyesters: poly(3-hydroxybutyrate-*co*-3-hydroxyvalerate) and poly(3-hydroxybutyrate-*co*-4-hydroxybutyrate), Macromolecules 23 (1990) 1933-1936.
[26] Y. Koga, H. Saito, Porous structure of crystalline polymers by exclusion effect of carbon dioxide, Polymer 47 (2006) 7564-7571.
[27] T. Oda, H. Saito, Exclusion effect of carbon dioxide on the crystallization of polypropylene, Journal of Polymer Science Part B: Polymer Physics 42 (2004) 1565-1572.
[28] N. Goldenfeld, Theory of spherulitic crystallization, Journal of Crystal Growth 84 (1987) 601-608.
[29] H.D. Keith, F.J. Padden, Jr., A Phenomenological theory of spherulitic crystallization, Journal of Applied Physics 34 (1963) 2409-2421.
[30] H.D. Keith, F.J. Padden, Jr., Spherulitic crystallization from the melt. I. Fractionation and impurity segregation and their influence on crystalline morphology, Journal of Applied Physics 35 (1964) 1270-1285.
[31] T. Okada, H. Saito, T. Inoue, Nonlinear crystal growth in the mixture of isotactic polypropylene and liquid paraffin, Macromolecules 23 (1990) 3865-3868.
[32] S.D. Hudson, D.D. Davis, A.J. Lovinger, Semicrystalline morphology of poly(aryl ether ether ketone)/poly(ether imide) blends, Macromolecules 25 (1992) 1759-1765.
[33] Y. Okabe, H. Murakami, N. Osaka, H. Saito, T. Inoue, Morphology development and exclusion of noncrystalline polymer during crystallization in PVDF/PMMA blends, Polymer 51 (2010) 1494-1500.
[34] H. Saito, B. Stühn, Exclusion of noncrystalline polymer from the interlamellar region in poly(vinylidene fluoride) / poly(methyl methacrylate) blends, Macromolecules 27 (1994) 216-218.
[35] R.S. Stein, F.B. Khambatta, F.P. Warner, T. Russell, A. Escala, E. Balizer, X-ray and optical studies of the morphology of polymer blends, Journal of Polymer Science: Polymer Symposium 63 (1978) 313-328.
[36] H.-J. Chiu, Miscibility and crystallization kinetics of poly(3-hydroxybutyrate-*co*-3-hydroxyvalerate)/poly(methyl methacrylate) blends, Journal of Applied Polymer Science 91 (2004) 3595-3603.
[37] H.-J. Chiu, Segregation morphology of poly(3-hydroxybutyrate)/poly(vinyl acetate) and poly(3-hydroxybutyrate-*co*-10% 3-hydroxyvalerate)/poly(vinyl acetate) blends as studied via small angle X-ray scattering, Polymer 46 (2005) 3906-3913.
[38] T.G. Ryan, P.D. Calvert, Diffusion and annealing in crystallizing polymers, Polymer 23 (1982) 877-883.
[39] Y.P. Handa, Z. Zhang, B. Wong, Effect of compressed CO_2 on phase transitions and polymorphism in syndiotactic polystyrene, Macromolecules 30 (1997) 8499-8504.
[40] E. Kiran, K. Liu, K. Ramsdell, Morphological changes in poly(ε-caprolactone) in dense carbon dioxide, Polymer 49 (2008) 1853-1859.
[41] Y.-T. Shieh, H.-S. Yang, Morphological changes of polycaprolactone with high-pressure CO_2 treatment, Journal of Supercritical Fluids 33 (2005) 183-192.

[42] H. Marubayashi, S. Akaishi, S. Akasaka, S. Asai, M. Sumita, Crystalline structure and morphology of poly(L-lactide) formed under high-pressure CO_2, Macromolecules 41 (2008) 9192-9203.
[43] G. Teramoto, T. Oda, H. Saito, H. Sano, Y. Fujita, Morphology control of polypropylene by crystallization under carbon dioxide, Journal of Polymer Science Part B: Polymer Physics 42 (2004) 2738-2746.
[44] Y. Doi, A. Tamaki, M. Kunioka, K. Soga, Production of copolyesters of 3-hydroxybutyrate and 3-hydroxyvalerate by Alcaligenes eutrophus from butyric and pentanoic acids, Applied Microbiology and Biotechnology 28 (1988) 330-334.
[45] P.A. Holmes, Applications of PHB - a microbially produced biodegradable thermoplastic, Physics in Technology 16 (1985) 32-36.
[46] A. Steinbüchel, H.E. Valentin, Diversity of bacterial polyhydroxyalkanoic acids, FEMS Microbiology Letters 128 (1995) 219-228.
[47] H. Bauer, A.J. Owen, Some structural and mechanical properties of bacterially produced poly-β-hydroxybutyrate-*co*-β-hydroxyvalerate, Colloid & Polymer Science 266 (1988) 241-247.
[48] S.J. Organ, P.J. Barham, Nucleation, growth and morphology of poly(hydroxybutyrate) and its copolymers, Journal of Materials Science 26 (1991) 1368-1374.
[49] M. Scandola, G. Ceccorulli, M. Pizzoli, M. Gazzano, Study of the crystal phase and crystallization rate of bacterial poly(3-hydroxybutyrate-*co*-3-hydroxyvalerate), Macromolecules 25 (1992) 1405-1410.
[50] Z. Wang, Y. Li, J. Yang, Q. Gou, Y. Wu, X. Wu, P. Liu, Q. Gu, Twisting of lamellar crystals in poly(3-hydroxybutyrate-*co*-3-hydroxyvalerate) ring-banded spherulites, Macromolecules 43 (2010) 4441-4444.
[51] H.-M. Ye, J.-S. Wang, S. Tang, J. Xu, X.-Q. Feng, B.-H. Guo, X.-M. Xie, J.-J. Zhou, L. Li, Q. Wu, G.-Q. Chen, Surface stress effects on the bending direction and twisting chirality of lamellar crystals of chiral polymer, Macromolecules 43 (2010) 5762-5770.
[52] Y. Jiang, J.-J. Zhou, L. Li, J. Xu, B.-H. Guo, Z.-M. Zhang, Q. Wu, G.-Q. Chen, L.-T. Weng, Z.-L. Cheung, C.-M. Chan, Surface properties of poly(3-hydroxybutyrate-*co*-3-hydroxyvalerate) banded spherulites studied by atomic force microscopy and time-flight secondary ion mass spectrometry, Langmuir 19 (2003) 7417-7422.
[53] Y. Furuhashi, H. Ito, T. Kikutani, T. Yamamoto, M. Kimizu, M. Cakmak, Structural analysis of poly(3-hydroxybutyrate-*co*-3-hydroxyvalerate) fibers prepared by drawing and annealing processes, Journal of Polymer Science Part B: Polymer Physics 36 (1998) 2471-2482.